

# Towards Efficient Visual Adaption via Structural Re-parameterization

Gen Luo<sup>1</sup>, Minglang Huang<sup>1</sup>, Yiyi Zhou<sup>12</sup>, Xiaoshuai Sun<sup>12</sup>, Guannan Jiang<sup>3</sup>, Zhiyu Wang<sup>3</sup>, Rongrong Ji<sup>12</sup>

<sup>1</sup>Media Analytics and Computing Lab, Department of Artificial Intelligence,  
School of Informatics, Xiamen University, 361005, China.

<sup>2</sup>Institute of Artificial Intelligence, Xiamen University, 361005, P.R. China.

<sup>3</sup>Intelligent Manufacturing Department, Contemporary Amperex Technology Co. Limited (CATL).

{luogen, huangminglang}@stu.xmu.edu.cn,

{zhouyiyi, xssun, rrji}@xmu.edu.cn, {jianggn, wangzy13}@catl.com

## Abstract

Parameter-efficient transfer learning (PETL) is an emerging research spot aimed at inexpensively adapting large-scale pre-trained models to downstream tasks. Recent advances have achieved great success in saving storage costs for various pre-trained models by updating a small number of parameters instead of full tuning. However, we notice that most existing PETL methods still incur non-negligible latency during inference. In this paper, we propose a parameter-efficient and computational friendly adapter for giant vision models, called RepAdapter. Specifically, we first prove that common adaptation modules can also be seamlessly integrated into most giant vision models via our structural re-parameterization, thereby achieving zero-cost during inference. We then investigate the sparse design and effective placement of adapter structure, helping our RepAdapter obtain other advantages in terms of parameter efficiency and performance. To validate RepAdapter, we conduct extensive experiments on 27 benchmark datasets of three vision tasks, i.e., image and video classifications and semantic segmentation. Experimental results show the superior performance and efficiency of RepAdapter than the state-of-the-art PETL methods. For instance, RepAdapter outperforms full tuning by +7.2% on average and saves up to 25% training time, 20% GPU memory, and 94.6% storage cost of ViT-B/16 on VTAB-1k. The generalization ability of RepAdapter is also well validated by a bunch of vision models. Our source code is released at <https://github.com/luogen1996/RepAdapter>.

## 1. Introduction

For a year or two, the research of large-scale pre-trained models has attracted an influx of interest from the computer

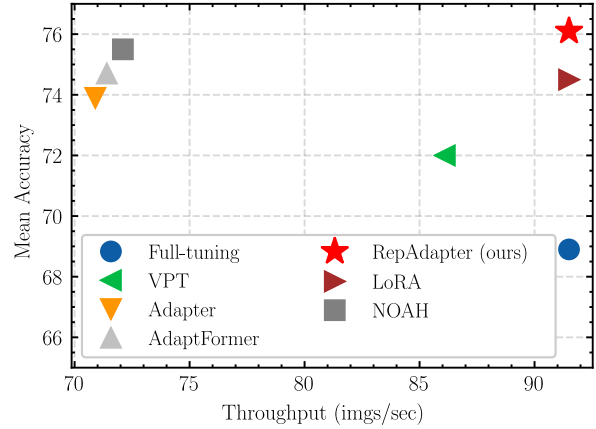


Figure 1. **Performance comparison of our RepAdapter and existing PETL methods [2, 16, 18, 19, 38] on VTAB-1K.** The vision model is ViT-B/16 and the inference speed is measured on a NVIDIA 3090 GPU with a batch size of 1. Most existing PETL methods incur non-negligible GPU latency during inference, while our RepAdapter does not.

vision community [11, 13, 29, 32, 36]. Alone with the outstanding performance on various vision tasks [3, 12, 21, 37, 41], large-scale pre-training also leads to a rapid growth in parameter size. In this case, directly fine-tuning these pre-trained models on downstream tasks, a common transfer learning strategy used before, becomes prohibitively expensive in terms of storage overhead. For instance, when fully fine-tuning ViT-G [36] on 19 vision tasks of VTAB-1k [37], it needs to store over 35 billion parameters for deployment.

To address this issue, numerous efforts have been recently devoted to *parameter-efficient transfer learning* (PETL) [2, 16, 18, 19, 22, 23, 25, 30, 31, 38, 40, 42, 43]. Inspired by the great success in natural language processing (NLP) [16, 18, 22, 23, 25, 30, 40], PETL methods for giant vision models also aim at reducing the tuning cost by updating or injecting a small fraction of parameters for each downstream task, which can be roughly divided into two

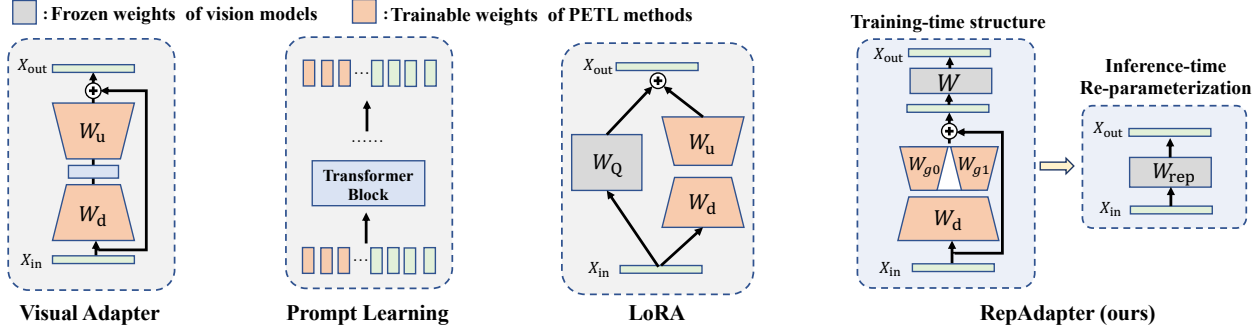


Figure 2. **Comparison of existing PETL methods [2, 18, 19] and our RepAdapter.** RepAdapter is deployed in a sequential manner, but it can be completely re-parameterized into the vision models during inference, enabling zero additional computational overhead. Its structure is also more lightweight than existing PETL methods.

main categories, namely *visual adapter* [2, 16, 20, 31, 38] and *prompt tuning* [19, 38, 42, 43]. Notably, very recent progresses also demonstrate competitive performance with lower parameter cost to full fine-tuning on Vision Transformers [2, 19, 38, 42, 43].

Despite the great success, most existing PETL methods inevitably slow down model inference [18], as shown in Fig. 1. For prompt-tuning methods [19, 42], the inserted tokens greatly increase the computation cost of vision models, especially the Transformer-based ones [11, 33]. In terms of visual adapters [2, 16], their theoretical cost is actually cheap, *e.g.*, +0.03 GFLOPs by the visual adapter [16]. But the modules they add also increase the network complexity, *e.g.*, the network depth, thus reducing the efficiency of GPU parallel computing. As shown in Fig. 1, when the batch size is 1, the latency of ViT [11] is increased by almost 20%, which is actually significant in real-world applications.

A trade-off solution is the newly proposed PETL method for pre-trained language models called *Low Rank Adaption* (LoRA) [18]. Inspired by the finding of the “low intrinsic rank” in large-scale pre-trained models [1], Hu *et al.* apply two decomposition matrices to approximate the projection weights of self-attention, as shown in Fig. 1. During inference, these weights can be re-parameterized into the pre-trained model, thereby avoiding additional computation. However, the generalization ability of LoRA is still limited for common vision models. For instance, when applying LoRA to CNN, *e.g.*, ConvNeXT [27], its performance is inferior to full tuning, *i.e.*, -1.9% on VTAB-1k [37]. On ViT [11], LoRA also performs worse than the adapter [2]. In addition, its re-parameterization is also not feasible for common adapters [16, 38] that are sequentially placed after neural modules.

In this paper, we investigate that whether common adaptation modules can be fully merged into the pre-trained models. In existing re-parameterization methods [6, 8, 10, 18], the merged parameters are all from the branch added in parallel, except the one for the re-parameterization of *norm* layer [24]. However, most visual adapters [16, 31, 38]

are deployed sequentially to directly optimize the feature spaces on downstream tasks, as shown in Fig. 2. In this paper, we find that when the adaptation module is linear, they can also be re-parameterized in a feed-forward structure without performance degeneration. This finding also allows us to keep the network intact during inference in addition to LoRA, while retaining the effectiveness of adapter.

Based on this finding, we further propose a novel PETL method called *RepAdapter*. As shown in Fig. 2, RepAdapter also inserts lightweight networks into the pre-trained models, and the additional parameters will be re-parameterized to the nearby projection weights after training. To the best of our knowledge, re-parameterization of this sequential structure is also the first attempt in the literature. In addition, we also investigate the sparse design of visual adapter and obtain a new dense-sparse structure, which can further save 25% parameters. Meanwhile, we empirically find that the adapter placement is essential for giant vision models.

To validate RepAdapter, we apply it to various vision models, ranging from CNNs like ConvNeXT [27] to single and multi-modal Transformers, *e.g.*, ViT [11] and CLIP [29]. Extensive experiments are conducted on 27 benchmark datasets of image and video classifications and semantic segmentation [3, 12, 14, 15, 21, 34, 37, 41]. Experimental results show that RepAdapter can outperform the state-of-the-art (SOTA) PETL methods [2, 19, 38, 43] in both performance and parameter size, while incurring no additional computations during inference. Meanwhile, we examine RepAdapter under the settings of few-shot learning and domain adaption, where its superior performance and generalizability still be also witnessed.

In summary, our contributions are three-fold:

- We propose a novel PETL method for vision models, called RepAdapter, which shows that common visual adapters can also be sequentially re-parameterized into pre-trained models.
- We investigate the sparse design and effective placement of visual adapter, which can further improve

RepAdapter in terms of parameter efficiency and performance.

- RepAdapter outperforms most existing PETL methods on 27 benchmarks of three vision tasks. Its generalization is validated on a wide range of vision models, including ConvNeXt, ViT, Swin-Transformer and CLIP.

## 2. Related Work

### 2.1. Parameter-efficient Transfer Learning

With the rapid growth of the model size, parameter-efficient transfer learning (PETL) has attracted increasing research interest [2, 16, 18, 19, 22, 23, 25, 30, 31, 38, 40, 42, 43]. PETL for large-scale pre-trained models first emerge in the field of natural language processing (NLP) [16, 18, 22, 23, 25, 30, 40], which demonstrates that only fine-tuning a few lightweight modules in a large-scale pre-trained models can achieve almost fully tuning performance. Drawing on the success experience in NLP, researchers have begun to apply the principle of PETL to large pre-trained vision models on various vision tasks [2, 16, 31, 38, 42, 43]. Among them, adapter-based [2, 16, 31] and prompt tuning based methods [42, 43] are two main paradigms for large-scale vision models. As illustrated in Fig. 2, adapter-based methods [2, 16, 31] insert small MLP networks into the vision model to adapt down-stream tasks. Prompt tuning [42, 43] is to add a few trainable tokens to the input sequence of vision Transformer to mitigate the gap between pre-training and downstream data distributions. LoRA [18] learns low-rank parameters for the frozen weights of multi-head attentions [33]. Zhang *et.al* [38] propose a prompt search algorithm to automatically combine the adapter, prompt tuning and LoRA together. Very recently, Lian *et. al* [24] insert normalization layers into vision models to adapt down-stream tasks, which can also be re-parameterized.

The principle of RepAdapter obviously differs from existing visual adapters [2, 16, 38] in its structure and placement. LoRA [18] and SSF [24] are two related methods, but their re-parameterizations are designed for simple modules like normalization layer [24]. Compared to these works, RepAdapter also demonstrates a better trade-off among performance, efficiency and generalization.

### 2.2. Structural Re-parameterization

Structural re-parameterization (SR) has achieved great success in designing efficient deep neural networks [5, 7, 9, 10]. The main target of existing SR methods is to convert a multi-branch structure to a single-branch one during inference. One representative SR work is RepVGG [10], which merges a multi-branch block with  $1 \times 1$  and  $3 \times 3$  convolution kernels and an identity layer into a single convolution layer, greatly reducing the computation overhead during inference. Inspired by RepVGG, DBBNet [8] proposes

an inception-like unit for ConvNet, which can be transformed to a convolution layer during inference. Similar work includes ACNet [6] and RepMLPNet [5], which effectively improves the model capacity via SR. Recently, some works [7, 9] find that SR benefits the training of large convolutional kernels [9] and the lossless pruning of CNN [7].

Our work is inspired from these progresses but also differs in two aspects. Firstly, our strategy is more flexible and can be deployed in common parameterized modules, *e.g.*, convolutions. Secondly, our RepAdapter is capable of re-parameterizing the sequential structures. Based on these two aspects, we believe that the proposed method is a viable complement to existing SR research.

## 3. Methods

### 3.1. Preliminary

We first revisit the visual adaption on a widely-used pre-trained model called Vision Transformer (ViT) [11].

**Vision Transformer.** Given an input image  $I \in \mathbb{R}^{H \times W \times 3}$ , ViT serializes it to visual tokens  $X \in \mathbb{R}^{n \times d}$  via patch embedding [11]. Then, a learnable token  $x_{cls} \in \mathbb{R}^{1 \times d}$  for classification is concatenated with  $X$ , and the positional embeddings  $P \in \mathbb{R}^{(n+1) \times d}$  are also added, which can be formulated by

$$X_0 = [x_{cls}, x_0, \dots, x_i] + P. \quad (1)$$

Afterwards, these visual inputs are processed by a set of Transformer layers, and the  $l$ -th block can be defined as

$$\begin{aligned} X'_l &= \text{MHA}(\text{LN}(X_{l-1})) + X_{l-1}, \\ X_l &= \text{FFN}(\text{LN}(X'_l)) + X'_l. \end{aligned} \quad (2)$$

MHA, FFN and LN denote the multi-head attention, feed-forward network and layer normalization, respectively.

In particular, MHA can be formulated by

$$\text{Attn}^i(X) = \text{softmax}\left(\frac{(XW_Q^i)(XW_K^i)^T}{\sqrt{d_k}}\right)(XW_V^i), \quad (3)$$

$$\text{MHA}(X) = [\text{Attn}^0(X), \dots, \text{Attn}^{n_h}(X)]W_O.$$

Here,  $\text{Attn}^i(X)$  is the *scale-dot* product attention for  $i$ -th head.  $[\cdot]$  denotes the concatenation operation.  $W_Q^i \in \mathbb{R}^{d \times \frac{d}{n_h}}$ ,  $W_K^i \in \mathbb{R}^{d \times \frac{d}{n_h}}$ ,  $W_V^i \in \mathbb{R}^{d \times \frac{d}{n_h}}$  and  $W_O \in \mathbb{R}^{d \times d}$  are the projection matrices. FFN can be defined as

$$\text{FFN}(X) = \sigma(XW_1 + b_1)W_2 + b_2, \quad (4)$$

where  $W_1 \in \mathbb{R}^{d \times 4d}$  and  $W_2 \in \mathbb{R}^{4d \times d}$  are two projection weights.  $b_1 \in \mathbb{R}^{4d}$  and  $b_2 \in \mathbb{R}^d$  are bias scalars.  $\sigma(\cdot)$  is the GELU function [4].

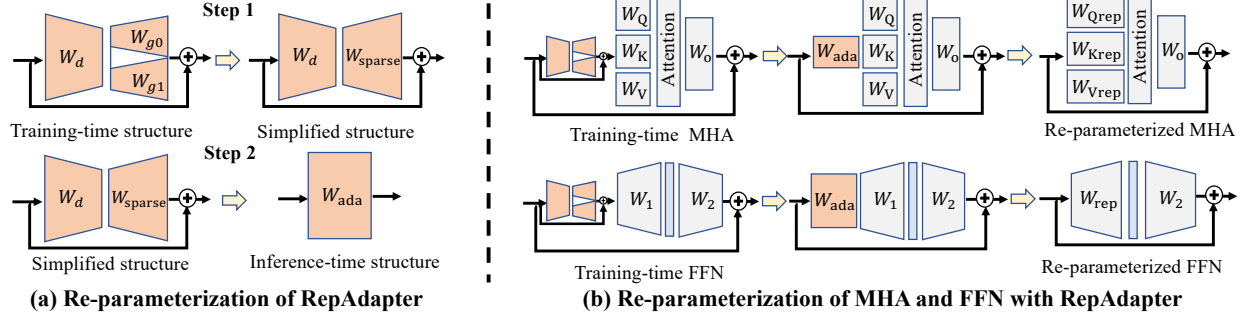


Figure 3. **Illustration the structural re-parameterization of RepAdapter.** (a) RepAdapter can be simplified to a linear projection after training. (b) The simplified weights can be merged into MHA and FFN.

**Visual Adapter.** Visual adapter is often a lightweight neural network with a bottleneck structure [2, 16] and a residual connection, which can be formulated by

$$f(X; \theta) = X + \phi_u(\sigma(\phi_d(X))). \quad (5)$$

Here,  $\sigma$  is the activation function,  $\phi_d$  and  $\phi_u$  denote the downsampling and upsampling projections, respectively.  $\phi$  is defined by  $\phi(X) = XW + b$ , where  $W \in \mathbb{R}^{d \times d'}$  and  $b \in \mathbb{R}^{d'}$  are the projection weight and bias, respectively. In practice, the hidden size of the adapter is very small, e.g., 8, which makes it very compact.

There are two common ways to deploy the adapter to Vision Transformers [2, 16]. The first one is the sequential manner [16], which places the adapter after FFN. Under this deployment, Eq. 2 can be modified by

$$X_l = f(\text{FFN}(\text{LN}(X'_l)); \theta) + X'_l. \quad (6)$$

The other one is the parallel deployment [2], where the adapter is placed to the FFN in parallel:

$$X_l = \text{FFN}(\text{LN}(X'_l)) + f(X'_l; \theta) + X'_l. \quad (7)$$

According to the principle of re-parameterization [6, 10], the parallel adapter can not be merged to Transformer due to the non-linearity of FFN. To the best of our knowledge, the re-parameterization for sequential adapters is also left unexplored in literature.

## 3.2. RepAdapter

### 3.2.1 Sequentially Structural Re-parameterization

We first propose a *sequentially structural re-parameterization* scheme towards zero extra cost during inference, which proves that common adapters can also be merged into the pre-trained model via simple tweaks.

Above all, we notice that most existing visual adapters [2, 31] involve a non-linear function in their structures, which is originally designed to improve the adaption on NLP tasks [16]. However, we find that removing the

non-linearity of adapters does not make performance degradation on vision tasks.

In this case, we first remove the non-linear function of visual adapter, and  $f(X; \theta)$  can be re-written as

$$f(X; \theta) = X + \phi_u(\phi_d(X)). \quad (8)$$

Here,  $\phi_u$  and  $\phi_d$  denote the dense projections in common adapters, and they can also be most linear transformations, e.g., the sparse layer in RepAdapter. During inference, the formulation  $f(X; \theta)$  of adapters is simplified to

$$\begin{aligned} f(X; \theta) &= (XW_d + b_d)W_u + b + X \\ &= XW_dW_u + XW_I + b_dW_u + b \\ &= XW_{\text{ada}} + b_{\text{ada}}. \end{aligned} \quad (9)$$

Here,  $W_d \in \mathbb{R}^{c \times d}$  and  $W_u \in \mathbb{R}^{c \times d}$  are the weight matrices.  $W_I \in \mathbb{R}^{d \times d}$  is an identity tensor.  $W_{\text{ada}} = W_dW_u + W_I$  and  $b_{\text{ada}} = b_dW_u + b$  are the re-parameterized weights and bias, respectively. In this way, we simplify the adapter structure to a linear projection layer, which can be incorporated into the near projection weights via matrix multiplications. Notably, Eq. 9 is also applicable for more complex structures, e.g., deep multi-layer network.

Based on Eq. 9, we depict the re-parameterization of adapters. When the adapter is sequentially placed into the vision model, we can re-parameterize  $f(X; \theta)$  into the pre-trained weight  $W_0$  and bias  $b_0$  by

$$\begin{aligned} \text{Rep}(f(X; \theta), W_0, b_0) &= f(X; \theta)W_0 + b_0 \\ &= XW_{\text{ada}}W_0 + b_{\text{ada}}W_0 + b_0 \\ &= XW_{\text{rep}} + b_{\text{rep}} \end{aligned} \quad (10)$$

Here,  $W_{\text{rep}} = W_{\text{ada}}W_0$  is the re-parameterized projection weights, and  $b_{\text{rep}} = b_{\text{ada}}W_0 + b_0$  is the re-parameterized bias term. In practice,  $W_0$  can also be the convolutional kernels, and we give its re-parameterization in appendix.

As shown in Fig. 3, we can incorporate common adapters into existing vision modules, e.g., MHA, FFN and convolutions, thereby avoiding additional inference costs.



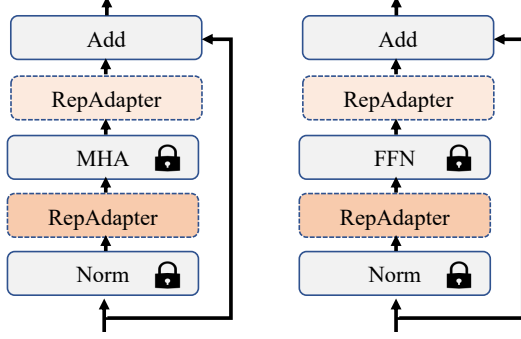


Figure 4. **The deployments of RepAdapter in ViT.** Four possible locations that RepAdapter can be inserted and re-parameterized. Our final deployments are in dark orange.

### 3.2.2 Adapter Structure

Next, we investigate the sparse structure of RepAdapter. Although the lightweight structure has been actively discussed in recent works [2, 16, 24, 38], we believe that it still has room to explore on vision models.

The first observation is that sparse transformation is a fundamental characteristic of many vision modules, *e.g.*, depthwise separable convolution [17]. Some research [35] also shows that sparse transformation can improve the model capacity for better performance. However, this property has yet to materialize in adapter.

Inspired by this, we propose a dense-to-sparse structure to RepAdapter, where  $\phi_u$  is formulated as a group-wise transformation [28] by

$$\phi_u(X) = [X'_{g0}W_{g0}, \dots, X'_{gk}W_{gk}] + b. \quad (11)$$

Here,  $X'_i \in \mathbb{R}^{n \times \frac{c}{k}}$  is the features splitted from  $X \in \mathbb{R}^{n \times c}$ ,  $k$  is the number of groups.  $W_i \in \mathbb{R}^{\frac{c}{k} \times \frac{d}{k}}$  is the projection weight matrix and  $b \in \mathbb{R}^d$  is the bias term. During inference,  $\phi_u(X)$  can also be converted to a dense projection layer via zero padding  $W_i$ . In this case, it can be re-parameterized with E.q 9 and 10.

This sparse design makes RepAdapter more lightweight than common visual adapters [2, 16], *e.g.*, saving about 25% parameters when the group number is 2.

**Adapter Placement.** Existing visual adapters [38] usually follow the deployment on pre-trained language models [16]. However, due to the great difference between visual and language models, we think that it is necessary to investigate the placement of adapters on vision models.

Considering that the parallel adapters are hard to re-parameterized, we investigate all possible sequential locations, as shown in Fig. 4. Empirically, we find that deploying RepAdapter before the neural modules can lead to better performance, which is also feasible for re-parameterization. Meanwhile, we also observe that it is more beneficial to apply RepAdapter to both MHA and FFN in ViT. These observations are further supported in our experiments.

Therefore, the deployment of RepAdapter in Transformer is

$$\begin{aligned} X'_l &= \text{MHA}(f(\text{LN}(X_{l-1}); \theta)) + X_{l-1}, \\ X_l &= \text{FFN}(f(\text{LN}(X'_l); \theta)) + X'_l. \end{aligned} \quad (12)$$

Notably, this deployment is also viable and effective for other vision models like CNN [27].

## 4. Experiments

### 4.1. Datasets and Metrics

**Image Classification.** VTb-1k benchmark contains 19 diverse image classification datasets, which are divided into three groups, *i.e.*, the *Natural*, *Specialized* and *Structured* groups, respectively. Each dataset contains 800 and 200 examples for training and validation, respectively. Following previous work [19, 38], we train models with all samples of *train* and *val* splits and report the top-1 accuracy on *test* split. ImageNet [3] is a large-scale image classification dataset with 1,000 categories. Following previous work [42, 43], we use 16 shots per category for few-shot learning. We evaluate domain generalization on the *val* set of ImageNet-Sketch [34], ImageNet-R [14] and ImageNet-A [15]. We report top-1 accuracy on their *val* set. Details about these datasets are reported in the appendix.

**Video Classification.** Something-Something V2 [12] is a large collection of video clips with 174 categories, which contains 169k videos for training and 20k videos for validation. HMDB51 [21] has 5k and 1.5k videos from 51 categories for training and validation, respectively. following [2], we report top-1 accuracy on *val* set.

**Semantic Segmentation.** ADE20K [41] is a challenging dataset for semantic segmentation, which has 20k and 2k images from 150 categories for training and validation. We report *mIoU* on its *val* set.

### 4.2. Implementation Details

For image classification, the default visual backbone is ViT-B/16 [11], which is pre-trained ImageNet-21k [3]. For video classification, we use ViT-B/16 pre-trained by VideoMAE [32] as the visual backbone. In terms of semantic segmentation, the visual backbone is ViT-L/14 pre-trained on ImageNet-21k. The hidden dimension  $c$  and the number of group  $k$  for RepAdapter is set to 8 and 2, respectively. The hyper-parameter  $s$  is searched from [0.1, 0.5, 1, 5, 10]. By default, we insert RepAdapter before MHA and FFN. We also provide a lightweight variant called **RepAdapter<sub>attn</sub>**, where the adapter is only deployed before MHA. Other details including image augmentation and hyper-parameters are kept the same with previous work [2, 19, 38, 42], which are provided in the appendix.

Table 1. **Comparison of RepAdapter and the state-of-the-arts PETL methods on VTAB-1k benchmark.** ViT-B/16 pretrained on ImageNet-21k is used as the vision model of all methods.

Model	Param (M)	Avg. Acc.	Natural							Specialized				Structured							
			Cifar100	Caltech101	DTD	Flower102	Pets	SVHN	Sun397	Camelyon	EuroSAT	Resisc45	Retinopathy	Clevr-Count	Clevr-Dist	DMLab	KITTI-Dist	dSpr-Loc	dSpr-Ori	sNORB-Azim	sNORB-Ele
Full tuning [19]	85.8	68.9	68.9	87.7	64.3	97.2	86.9	87.4	38.8	79.7	95.7	84.2	73.9	56.3	58.6	41.7	65.5	57.5	46.7	25.7	29.1
Linear probe [19]	0.04	57.6	64.4	85.0	63.2	97.0	86.3	36.6	51.0	78.5	87.5	68.5	74.0	34.3	30.6	33.2	55.4	12.5	20.0	9.6	19.2
Adapter [16]	0.16	73.9	69.2	90.1	68.0	98.8	89.9	82.8	54.3	84.0	94.9	81.9	75.5	80.9	65.3	48.6	78.3	74.8	<b>48.5</b>	29.9	41.6
AdaptFormer [2]	0.16	74.7	<b>70.8</b>	<b>91.2</b>	70.5	<b>99.1</b>	<b>90.9</b>	86.6	<b>54.8</b>	83.0	<b>95.8</b>	84.4	<b>76.3</b>	<b>81.9</b>	64.3	49.3	80.3	<b>76.3</b>	45.7	<b>31.7</b>	41.1
RepAdapter <sub>attn</sub>	0.11	<b>75.5</b>	70.7	<b>91.6</b>	<b>72.5</b>	<b>99.1</b>	91.3	<b>88.5</b>	54.2	<b>84.1</b>	95.7	<b>85.1</b>	74.6	81.6	<b>69.1</b>	<b>50.4</b>	<b>81.9</b>	<b>79.5</b>	45.6	<b>34.6</b>	<b>41.9</b>
VPT [19]	0.53	72.0	<b>78.8</b>	90.8	65.8	98.0	88.3	78.1	49.6	81.8	<b>96.1</b>	83.4	68.4	68.5	60.0	46.5	72.8	73.6	47.9	<b>32.9</b>	37.8
LoRA [18]	0.29	74.5	67.1	91.4	69.4	98.8	90.4	85.3	<b>54.0</b>	84.9	95.3	84.4	73.6	<b>82.9</b>	<b>69.2</b>	49.8	78.5	75.7	47.1	31.0	44.0
NOAH [38]	0.36	75.5	69.6	<b>92.7</b>	70.2	99.1	90.4	86.1	53.7	84.4	95.4	83.9	<b>75.8</b>	82.8	68.9	49.9	<b>81.7</b>	<b>81.8</b>	48.3	32.8	<b>44.2</b>
SSF [24]	0.24	75.7	69.0	92.6	<b>75.1</b>	<b>99.4</b>	<b>91.8</b>	90.2	52.9	<b>87.4</b>	95.9	<b>87.4</b>	75.5	75.9	62.3	<b>53.3</b>	80.6	77.3	<b>54.9</b>	29.5	37.9
RepAdapter	0.22	<b>76.1</b>	72.4	91.6	71.0	99.2	91.4	<b>90.7</b>	<b>55.1</b>	85.3	95.9	84.6	<b>75.9</b>	82.3	68.0	50.4	79.9	80.4	49.2	<b>38.6</b>	41.0

Table 2. **Ablation studies on VTAB-1k.** The base model is ViT-B/16, and the default setting is RepAdapter<sub>attn</sub>, which only has an adapter before MHA. “Avg acc” denotes the average accuracy on VTAB-1k. “Act.” denotes the use of activation functions. “Parallel” denotes that RepAdapter is placed in parallel to MHA. “Full sparse” means that all projections are group-wise. The best settings are in gray.

(a) Number of groups.			(b) Hidden dimensions.			(c) Adapter position.		(d) Adapter variants.	
groups	params	avg acc.	dims	params	avg acc.	position	avg acc.	setting	avg acc.
1	0.16M	75.3	4	0.05M	74.4	before attn	<b>75.5</b>	default	<b>75.5</b>
2	0.11M	<b>75.5</b>	8	0.11M	<b>75.5</b>	after attn	74.9	w.i. act.	75.5
4	0.09M	74.9	12	0.16M	75.3	before mlp	75.2	parallel [2]	75.2
8	0.08M	74.5	16	0.22M	75.1	after mlp	74.6	full sparse	75.1

Table 3. **Cumulative ablation of RepAdapter<sub>attn</sub> on VTAB-1k.** We use ViT-B/16 as the base model.

Settings	Param (M)	Avg Acc.
Baseline (Adapter [16])	0.16	73.9
+ dense-sparse transformations	0.11	74.5
+ pre-insertion	0.11	75.5
+ linear structure	0.11	75.5

### 4.3. Experimental Results

#### 4.3.1 Comparisons with the State-of-the-arts.

We first compare RepAdapter with the state-of-the-art (SOTA) PETL methods on ViT, as reported in Tab. 1. We first observe that all PETL methods outperform full fine-tuning by a large margin, while linear probing, only tuning the classifier, performs much worse. These results confirm the effectiveness of PETL methods for ViT. Compared to these approaches, we can see that RepAdapter performs much better on VTAB-1k, *e.g.*, +0.7% on Resisc45. In particular, RepAdapter<sub>attn</sub> can achieve SOTA performance while being much more lightweight than all PETL approaches, *i.e.*, 0.11M. When employing RepAdapter in both MHA and FFN, the average performance can be further improved from 75.5 to 76.1, which outperforms the SOTA ap-

proach NOAH [38] by +0.6%. Compared to LoRA [18], which is also zero-cost during inference, RepAdapter also merits in performance and efficiency, *e.g.*, +1.6% average accuracy. These results greatly validate the effectiveness and parameter efficiency of the proposed RepAdapter.

#### 4.3.2 Ablation Studies

To gain deep insights into RepAdapter, we conduct extensive ablation studies in Tab. 2 - 3. In Tab. 3, we validate the effectiveness of each designs in RepAdapter. From this table, the first observation is that the sparse structure and the new placement obtains obvious improvements on ViT-B/16, resulting in +0.6% and +1.0% accuracy, respectively. Meanwhile, We see that activation function is less important under our settings. Overall, these results validate the benefits of RepAdapter’s designs on vision models.

In Tab. 2a, we show the impacts of group number. When the number of groups is set to 1, RepAdapter is actually a dense network. Notably, this dense structure does not perform best with more parameters. Instead, increasing a certain number of groups is beneficial to both performance and efficiency. Similar results can be found in Tab. 2b, which shows the impact of parameter size. We observe that more parameters for RepAdapter do not always improve perfor-

Table 4. **Efficiency comparison of RepAdapter and existing PETL methods during inference.** We use ViT-B/16 as the vision model.  $\Delta P$  and  $\Delta F$  denote the additional parameters and FLOPs by PETL methods. The inference speed is defined by images per second (imgs/sec) and measured on a NVIDIA 3090 GPU. All results are the average of 100 trials.

Methods	$\Delta P$	$\Delta F$	GPU latency (imgs/sec)			
			bs=1	bs=4	bs=16	bs=128
Full tuning	0	0	91.5	375.7	539.5	578.3
VPT [19] <sup>2</sup>	0.55M	5.60G	86.1 (-5.9%)	283.5 (-24.5%)	381.5 (-29.2%)	421.6 (-27.1%)
Adapter [16]	0.16M	0.03G	70.9 (-22.5%)	306.6 (-18.3%)	504.7 (-6.4%)	552.4 (-5.8%)
AdaptFormer [2]	0.16M	0.03G	71.4 (-21.9%)	309.9 (-17.5%)	508.1 (-4.2%)	555.2 (-3.9%)
NOAH [38] <sup>2</sup>	0.12M	0.02G	72.1 (-21.2%)	312.7 (-16.7%)	492.9 (-8.6%)	534.7 (-7.5%)
RepAdapter (ours)	0	0	91.5 (-0.0%)	375.7 (-0.0%)	539.5 (-0.0%)	578.3 (-0.0%)

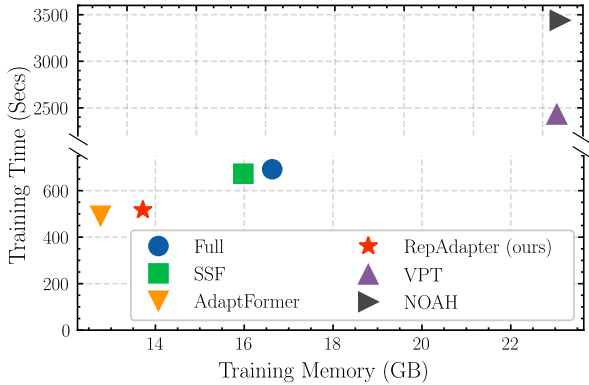


Figure 5. **Comparisons of training time and memory overhead on a NVIDIA A100 GPU.**

mance, which may attribute to the overfitting problem on small-scale downstream datasets, which also suggests the superiority of our sparse design. Tab. 2c shows the impact of deployment location. It can be seen that the pre-insertion is consistently better than the post-insertion, while the later is more commonly used [16, 31]. In Tab. 2d, we compare RepAdapter to its three variants. We can see that the parallel adapters like like AdaptFormer [2] is worse than RepAdapter. Besides, the fully sparse structure declines performance, suggesting the importance of RepAdapter’s dense part for information exchange. Overall, these results well validate the design of RepAdapter.

### 4.3.3 Efficiency Analysis

In Tab. 4, we compare the inference speed with RepAdapter and existing PETL methods. Compared to RepAdapter, four recent PETL approaches all slow down the inference to different degrees. For example, Adapter [16] is slower than RepAdapter by 22.5% when batch size is 1. However, the extra computation it brings is only 0.03 GFLOPs. To explain, FLOPs reflect the complexity for CPU computing. But in practice, GPU latency is also affected by the network topology, *e.g.*, the network depth. In this case, we can see that the additional FLOPs of visual prompt tuning

(VPT) [19] are up to 5.6G, but its latency is smaller than visual adapters when the batch size is 1.

In Fig. 5, we further compare the training costs of these PETL methods. The first observation is that VPT [19] and NOAH [38] consume much more training costs. For example, due to the super-network training and sub-network search, NOAH requires about  $5\times$  training time and  $1.4\times$  GPU memories than full fine-tuning. Compared to full tuning, RepAdapter reduces about 25% training time and 20% GPU memory of full tuning, well confirming its efficiency.

### 4.3.4 Generalization Experiments

**Few-shot learning and domain generalization.** We further apply RepAdapter to CLIP [29] and validate it on few-show learning and domain generalization, as shown in Tab. 5. We provide two different setups for CLIP, *i.e.*, RepAdapter-V and RepAdapter-T, which deploy RepAdapter in the visual and text encoders, respectively. Compared to zero-shot CLIP [29], both RepAdapter-V and RepAdapter-T can improve the performance on the source and target datasets, *e.g.*, +3.77% on ImageNet-A. Notably, RepAdapter-T even outperforms the SOTA soft-prompt approach, *i.e.*, CoCoOp [43], by using a simple hand-craft prompt of “a photo of a [CLASS]”.

**Results of more network architectures.** In Tab. 6, we deploy RepAdapter to more vision models including ConvNeXt [27] and Swin-Transformer [26]. We compare RepAdapter with three baselines on VT-B-1k, *i.e.*, full fine-tuning, linear probing and VPT. From Tab. 6, we can first see that linear probing performs much worse than full fine-tuning on all models. Besides, we also find that the generalization of VPT and LoRA is poor on the non-Transformer network, *i.e.*, ConvNeXt [27]. The performance is about 5.3% lower than full fine-tuning. In stark contrast, our RepAdapter achieves significant performance gains over full fine-tuning on all models, *e.g.*, +5% on ConvNeXt,

<sup>2</sup>The module dimensions of VPT and NOAH are different across datasets, so we use the averaged dimensions to measure their latency.

Table 5. **Results of adapting CLIP to 16-shot ImageNet classification and domain generalization.** ViT-B/16 is used as the visual backbone. RepAdapter-V and RepAdapter-T denote the adaptations to the visual and text encoders of CLIP, respectively. The handcraft prompt of “a photo of a [CLASS]” is used for tuning.

Method	Source	Target			
	ImageNet	-V2	-S	-A	-R
Zero-shot [29]	66.73	60.83	46.15	47.77	73.96
CoOp [42]	<u>71.51</u>	64.20	47.99	49.71	75.21
CoCoOp [43]	71.02	<u>64.07</u>	<u>48.75</u>	<u>50.63</u>	<u>76.18</u>
RepAdapter-V	70.93	64.00	48.40	45.53	75.77
RepAdapter-T	<b>71.87</b>	<b>64.77</b>	<b>49.30</b>	<b>51.13</b>	<b>76.47</b>

Table 6. **Results of RepAdapter on different network architectures on VTAB-1k.** “Avg” denotes the average accuracy. “Nat”, “Spe” and “Str” are the average accuracies of the natural, specialized and structured groups, respectively.

Model	Method	Avg.	Nat.	Spe.	Str.
<i>Convolutional Network:</i>					
ConvNeXt-B	Full	<u>74.0</u>	78.0	<u>83.7</u>	<u>60.4</u>
ConvNeXt-B	Linear	63.6	74.5	81.5	34.8
ConvNeXt-B	VPT	68.7	78.5	83.0	44.6
ConvNeXt-B	LoRA	72.1	<u>79.2</u>	83.4	53.8
ConvNeXt-B	RepAdapter	<b>79.0</b>	<b>83.5</b>	<b>86.7</b>	<b>66.8</b>
<i>Hierarchical Vision Transformer:</i>					
Swin-B	Full	<u>75.0</u>	<u>79.2</u>	<u>86.2</u>	<u>59.7</u>
Swin-B	Linear	62.6	73.5	80.8	33.5
Swin-B	VPT	71.6	76.8	84.5	53.4
Swin-B	RepAdapter	<b>77.4</b>	<b>82.7</b>	<b>87.5</b>	<b>62.0</b>
<i>Vision Transformer:</i>					
ViT-B/16	Full	68.9	75.9	<u>83.4</u>	47.6
ViT-B/16	Linear	57.6	68.9	77.2	26.8
ViT-B/16	VPT	<u>72.0</u>	<u>78.5</u>	82.4	<u>55.0</u>
ViT-B/16	RepAdapter	<b>76.0</b>	<b>81.6</b>	<b>85.4</b>	<b>61.2</b>

Table 7. **Comparisons of RepAdapter and the state-of-the-arts PETL methods on video classification.** For all methods, the backbone is ViT-B/16 pre-trained by VideoMAE [32]. We report top-1 accuracy on val set.

Method	Params (M)	SSv2	HMDB51
Full tuning [32]	86.04	53.97	46.41
Linear probe [32]	0.07	29.23	49.84
VPT [19]	0.08	43.73	52.67
AdaptFormer-1 [2]	0.10	50.03	51.68
AdaptFormer-4 [2]	0.15	54.70	51.81
AdaptFormer-64 [2]	1.26	<u>59.02</u>	<u>55.69</u>
RepAdapter-2	0.15	55.26	55.67
RepAdapter-16	0.53	<b>60.52</b>	<b>59.21</b>

strongly confirming its generalization ability.

Table 8. **Results of RepAdapter on semantic segmentation.** SETR [39] is the vision model, and we report its mIoU scores on ADE20K [41] val set. “mIoU-SS” and “mIoU-MS” denote the results of single- and multi-scale predictions, respectively.

Methods	Params (M)	mIoU-SS	mIoU-MS
Full tuning [39]	318.31	<u>48.31</u>	<u>50.07</u>
Head only [39]	13.18	35.12	37.46
Bias [19]	13.46	43.40	45.33
VPT [19]	13.43	42.11	44.06
VPT + Bias [19]	15.79	44.04	45.63
RepAdapter	13.82	<b>44.44</b>	<b>46.71</b>

**Results of more vision tasks.** In Tab. 7, we compare RepAdapter with VPT [19] and AdaptFormer [2] on video classification. The first observation is that video classification is difficult for VPT, so its accuracy is inferior to full tuning on SSv2 [12]. Meanwhile, we find that AdaptFormer can outperform full tuning with much fewer parameters, and its best performance only requires 1.26M parameters. Even so, RepAdapter is consistently better than AdaptFormer at similar parameter scales. For example, RepAdapter-16 outperforms AdaptFormer-64 by +3.52% on HMDB51 while saving more than 50% parameters.

Afterwards, we validate RepAdapter on SETR [39] for semantic segmentation in Tab. 8. This adaptation is challenging due to the huge gap between the objectives of pre-training and downstream tasks. In this case, we can see that only fine-tuning the head results in very poor performance, *i.e.*, -13.19% mIoU-SS. Meanwhile, the performance of VPT is still inferior than tuning bias (Bias). Compared to these approaches, RepAdapter demonstrates better adaptations. With less parameters, RepAdapter outperforms the best PETL solution “VPT+Bias” by +1.08 mIoU under the multi-scale prediction setting (mIoU-MS).

## 5. Conclusions

In this paper, we focus on *parameter efficient transfer learning* (PETL) for giant vision models and propose a novel PETL method, termed RepAdapter. The most outstanding property of RepAdapter is that its parameters can be completely merged into the pre-trained vision model via structural re-parameterization, thereby incurring zero extra costs during inference. In addition, RepAdapter is still more effective than existing PETL approaches due to its novel sparse structure and our careful deployment. To validate RepAdapter, we apply it to a set of large vision models and conduct extensive experiments on 27 datasets of three vision tasks. Experimental results well confirm its superiority in terms of efficiency, performance and generalization.



**Acknowledgements.** This work was supported by the National Science Fund for Distinguished Young Scholars (No.62025603), the National Natural Science Foundation of China (No. U21B2037, No. U22B2051, No. 62176222, No. 62176223, No. 62176226, No. 62072386, No. 62072387, No. 62072389, No. 62002305 and No. 62272401), Guangdong Basic and Applied Basic Research Foundation (No.2019B1515120049), and the Natural Science Foundation of Fujian Province of China (No.2021J01002, No.2022J06001).

## References

- [1] Armen Aghajanyan, Luke Zettlemoyer, and Sonal Gupta. Intrinsic dimensionality explains the effectiveness of language model fine-tuning. *arXiv preprint arXiv:2012.13255*, 2020. [2](#)
- [2] Shoufa Chen, Chongjian Ge, Zhan Tong, Jiangliu Wang, Yibing Song, Jue Wang, and Ping Luo. Adaptformer: Adapting vision transformers for scalable visual recognition. *CoRR*, abs/2205.13535, 2022. [1](#), [2](#), [3](#), [4](#), [5](#), [6](#), [7](#), [8](#)
- [3] Jia Deng, Wei Dong, Richard Socher, Li-Jia Li, Kai Li, and Li Fei-Fei. Imagenet: A large-scale hierarchical image database. In *CVPR*, 2009. [1](#), [2](#), [5](#)
- [4] Jacob Devlin, Ming-Wei Chang, Kenton Lee, and Kristina Toutanova. BERT: pre-training of deep bidirectional transformers for language understanding. In *NAACL-HLT*, 2019. [3](#)
- [5] Xiaohan Ding, Honghao Chen, Xiangyu Zhang, Jungong Han, and Guiguang Ding. Repmlpnet: Hierarchical vision mlp with re-parameterized locality. In *Proceedings of the IEEE/CVF Conference on Computer Vision and Pattern Recognition*, pages 578–587, 2022. [3](#)
- [6] Xiaohan Ding, Yuchen Guo, Guiguang Ding, and Jungong Han. Acnet: Strengthening the kernel skeletons for powerful cnn via asymmetric convolution blocks. In *Proceedings of the IEEE/CVF international conference on computer vision*, pages 1911–1920, 2019. [2](#), [3](#), [4](#)
- [7] Xiaohan Ding, Tianxiang Hao, Jianchao Tan, Ji Liu, Jungong Han, Yuchen Guo, and Guiguang Ding. Resrep: Lossless cnn pruning via decoupling remembering and forgetting. In *Proceedings of the IEEE/CVF International Conference on Computer Vision*, pages 4510–4520, 2021. [3](#)
- [8] Xiaohan Ding, Xiangyu Zhang, Jungong Han, and Guiguang Ding. Diverse branch block: Building a convolution as an inception-like unit. In *Proceedings of the IEEE/CVF Conference on Computer Vision and Pattern Recognition*, pages 10886–10895, 2021. [2](#), [3](#)
- [9] Xiaohan Ding, Xiangyu Zhang, Jungong Han, and Guiguang Ding. Scaling up your kernels to 31x31: Revisiting large kernel design in cnns. In *Proceedings of the IEEE/CVF Conference on Computer Vision and Pattern Recognition*, pages 11963–11975, 2022. [3](#)
- [10] Xiaohan Ding, Xiangyu Zhang, Ningning Ma, Jungong Han, Guiguang Ding, and Jian Sun. Repvgg: Making vgg-style convnets great again. In *Proceedings of the IEEE/CVF Conference on Computer Vision and Pattern Recognition*, pages 13733–13742, 2021. [2](#), [3](#), [4](#)
- [11] Alexey Dosovitskiy, Lucas Beyer, Alexander Kolesnikov, Dirk Weissenborn, Xiaohua Zhai, Thomas Unterthiner, Mostafa Dehghani, Matthias Minderer, Georg Heigold, Sylvain Gelly, Jakob Uszkoreit, and Neil Houlsby. An image is worth 16x16 words: Transformers for image recognition at scale. In *ICLR*, 2021. [1](#), [2](#), [3](#), [5](#)
- [12] Raghav Goyal, Samira Ebrahimi Kahou, Vincent Michalski, Joanna Materzynska, Susanne Westphal, Heuna Kim, Valentin Haenel, Ingo Fruend, Peter Yianilos, Moritz Mueller-Freitag, et al. The” something something” video database for learning and evaluating visual common sense. In *Proceedings of the IEEE international conference on computer vision*, pages 5842–5850, 2017. [1](#), [2](#), [5](#), [8](#)
- [13] Kaiming He, Xinlei Chen, Saining Xie, Yanghao Li, Piotr Dollár, and Ross B. Girshick. Masked autoencoders are scalable vision learners. In *CVPR*, 2022. [1](#)
- [14] Dan Hendrycks, Steven Basart, Norman Mu, Saurav Kadavath, Frank Wang, Evan Dorundo, Rahul Desai, Tyler Zhu, Samyak Parajuli, Mike Guo, et al. The many faces of robustness: A critical analysis of out-of-distribution generalization. In *Proceedings of the IEEE/CVF International Conference on Computer Vision*, pages 8340–8349, 2021. [2](#), [5](#)
- [15] Dan Hendrycks, Kevin Zhao, Steven Basart, Jacob Steinhardt, and Dawn Song. Natural adversarial examples. In *Proceedings of the IEEE/CVF Conference on Computer Vision and Pattern Recognition*, pages 15262–15271, 2021. [2](#), [5](#)
- [16] Neil Houlsby, Andrei Giurgiu, Stanislaw Jastrzebski, Bruna Morrone, Quentin de Laroussilhe, Andrea Gesmundo, Mona Attariyan, and Sylvain Gelly. Parameter-efficient transfer learning for NLP. In *ICML*, 2019. [1](#), [2](#), [3](#), [4](#), [5](#), [6](#), [7](#)
- [17] Andrew G Howard, Menglong Zhu, Bo Chen, Dmitry Kalenichenko, Weijun Wang, Tobias Weyand, Marco Andreetto, and Hartwig Adam. Mobilenets: Efficient convolutional neural networks for mobile vision applications. *arXiv preprint arXiv:1704.04861*, 2017. [5](#)
- [18] Edward J Hu, yelong shen, Phillip Wallis, Zeyuan Allen-Zhu, Yanzhi Li, Shean Wang, Lu Wang, and Weizhu Chen. LoRA: Low-rank adaptation of large language models. In *ICLR*, 2022. [1](#), [2](#), [3](#), [6](#)
- [19] Menglin Jia, Luming Tang, Bor-Chun Chen, Claire Cardie, Serge J. Belongie, Bharath Hariharan, and Ser-Nam Lim. Visual prompt tuning. In *ECCV*, 2022. [1](#), [2](#), [3](#), [5](#), [6](#), [7](#), [8](#)
- [20] Shibo Jie and Zhi-Hong Deng. Convolutional bypasses are better vision transformer adapters. *arXiv preprint arXiv:2207.07039*, 2022. [2](#)
- [21] Hildegard Kuehne, Hueihan Jhuang, Estíbaliz Garrote, Tomaso Poggio, and Thomas Serre. Hmdb: a large video database for human motion recognition. In *2011 International conference on computer vision*, pages 2556–2563. IEEE, 2011. [1](#), [2](#), [5](#)
- [22] Brian Lester, Rami Al-Rfou, and Noah Constant. The power of scale for parameter-efficient prompt tuning. *arXiv preprint arXiv:2104.08691*, 2021. [1](#), [3](#)

- [23] Xiang Lisa Li and Percy Liang. Prefix-tuning: Optimizing continuous prompts for generation. In *ACL/IJCNLP*, 2021. 1, 3
- [24] Dongze Lian, Daquan Zhou, Jiashi Feng, and Xinchao Wang. Scaling & shifting your features: A new baseline for efficient model tuning. In *Advances in Neural Information Processing Systems (NeurIPS)*, 2022. 2, 3, 5, 6
- [25] Pengfei Liu, Weizhe Yuan, Jinlan Fu, Zhengbao Jiang, Hiroaki Hayashi, and Graham Neubig. Pre-train, prompt, and predict: A systematic survey of prompting methods in natural language processing. *arXiv preprint arXiv:2107.13586*, 2021. 1, 3
- [26] Ze Liu, Yutong Lin, Yue Cao, Han Hu, Yixuan Wei, Zheng Zhang, Stephen Lin, and Baining Guo. Swin transformer: Hierarchical vision transformer using shifted windows. In *ICCV*, 2021. 7
- [27] Zhuang Liu, Hanzi Mao, Chao-Yuan Wu, Christoph Feichtenhofer, Trevor Darrell, and Saining Xie. A convnet for the 2020s. In *CVPR*, 2022. 2, 5, 7
- [28] Gen Luo, Yiyi Zhou, Xiaoshuai Sun, Yan Wang, Liujuan Cao, Yongjian Wu, Feiyue Huang, and Rongrong Ji. Towards lightweight transformer via group-wise transformation for vision-and-language tasks. *IEEE Transactions on Image Processing*, 31:3386–3398, 2022. 5
- [29] Alec Radford, Jong Wook Kim, Chris Hallacy, Aditya Ramesh, Gabriel Goh, Sandhini Agarwal, Girish Sastry, Amanda Askell, Pamela Mishkin, Jack Clark, Gretchen Krueger, and Ilya Sutskever. Learning transferable visual models from natural language supervision. In *ICML*, Proceedings of Machine Learning Research, 2021. 1, 2, 7, 8
- [30] Taylor Shin, Yasaman Razeghi, Robert L Logan IV, Eric Wallace, and Sameer Singh. Autoprompt: Eliciting knowledge from language models with automatically generated prompts. *arXiv preprint arXiv:2010.15980*, 2020. 1, 3
- [31] Yi-Lin Sung, Jaemin Cho, and Mohit Bansal. Vi-adapter: Parameter-efficient transfer learning for vision-and-language tasks. In *Proceedings of the IEEE/CVF Conference on Computer Vision and Pattern Recognition*, pages 5227–5237, 2022. 1, 2, 3, 4, 7
- [32] Zhan Tong, Yibing Song, Jue Wang, and Limin Wang. Videomae: Masked autoencoders are data-efficient learners for self-supervised video pre-training. *arXiv preprint arXiv:2203.12602*, 2022. 1, 5, 8
- [33] Ashish Vaswani, Noam Shazeer, Niki Parmar, Jakob Uszkoreit, Llion Jones, Aidan N. Gomez, Lukasz Kaiser, and Illia Polosukhin. Attention is all you need. In *NIPS*, 2017. 2, 3
- [34] Haohan Wang, Songwei Ge, Zachary Lipton, and Eric P Xing. Learning robust global representations by penalizing local predictive power. *Advances in Neural Information Processing Systems*, 32, 2019. 2, 5
- [35] Saining Xie, Ross Girshick, Piotr Dollár, Zhuowen Tu, and Kaiming He. Aggregated residual transformations for deep neural networks. In *Proceedings of the IEEE conference on computer vision and pattern recognition*, pages 1492–1500, 2017. 5
- [36] Xiaohua Zhai, Alexander Kolesnikov, Neil Houlsby, and Lucas Beyer. Scaling vision transformers. In *CVPR*, 2022. 1
- [37] Xiaohua Zhai, Joan Puigcerver, Alexander Kolesnikov, Pierre Ruysen, Carlos Riquelme, Mario Lucic, Josip Djolonga, André Susano Pinto, Maxim Neumann, Alexey Dosovitskiy, Lucas Beyer, Olivier Bachem, Michael Tschannen, Marcin Michalski, Olivier Bousquet, Sylvain Gelly, and Neil Houlsby. The visual task adaptation benchmark. *CoRR*, abs/1910.04867, 2019. 1, 2
- [38] Yuanhan Zhang, Kaiyang Zhou, and Ziwei Liu. Neural prompt search. *CoRR*, abs/2206.04673, 2022. 1, 2, 3, 5, 6, 7
- [39] Sixiao Zheng, Jiachen Lu, Hengshuang Zhao, Xiatian Zhu, Zekun Luo, Yabiao Wang, Yanwei Fu, Jianfeng Feng, Tao Xiang, Philip HS Torr, et al. Rethinking semantic segmentation from a sequence-to-sequence perspective with transformers. In *Proceedings of the IEEE/CVF conference on computer vision and pattern recognition*, pages 6881–6890, 2021. 8
- [40] Zexuan Zhong, Dan Friedman, and Danqi Chen. Factual probing is [mask]: Learning vs. learning to recall. *arXiv preprint arXiv:2104.05240*, 2021. 1, 3
- [41] Bolei Zhou, Hang Zhao, Xavier Puig, Tete Xiao, Sanja Fidler, Adela Barriuso, and Antonio Torralba. Semantic understanding of scenes through the ade20k dataset. *International Journal of Computer Vision*, 127(3):302–321, 2019. 1, 2, 5, 8
- [42] Kaiyang Zhou, Jingkan Yang, Chen Change Loy, and Ziwei Liu. Learning to prompt for vision-language models. *CoRR*, abs/2109.01134, 2021. 1, 2, 3, 5, 8
- [43] Kaiyang Zhou, Jingkan Yang, Chen Change Loy, and Ziwei Liu. Conditional prompt learning for vision-language models. In *CVPR*, 2022. 1, 2, 3, 5, 7, 8